SEBASTIAN KORNET[a,b1] and JANUSZ BADUR[a]

Enhanced evaporation of the condensate droplets within the asymmetrical shock wave zone

[a] Energy Conversion Department, The Szewalski Institute of Fluid-Flow Machinery of the Polish Academy of Sciences, Fiszera 14, 80-231 Gdańsk, Poland

[b] Conjoint Doctoral School at the Faculty of Mechanical Engineering, Gdańsk University of Technology, Narutowicza 11/12, 80-233 Gdańsk, Poland

Abstract

The present work is concerned with investigation into coupled phenomena occurring in the supersonic section of the de Laval nozzle, characterized by the presence of shock the flow of condensing steam. The numerical simulations results were compared with the experiment carried out by Dykas et al. in 2013 on the half arc nozzles. The present work includes simulations results of oscillation frequency of the shock wave and conditions for the enhancement evaporation of condensate within the asymmetrical shock wave. Novelty of our approach lies on modeling both the moment of initiation of a phase transition, as well as the moment of its reverse progress – called here revaporization of the condensate phase.

Keywords: Revaporization; Shock wave; Homogenous condensation; Asymmetrical lambda foot

Nomenclature

a	–	number of droplets per unit volume
$\mathbf{b} = -9.81\mathbf{e}_z$	–	mass force of Earth gravity

---

[1]Corresponding author. E-mail address: sebastian.kornet@imp.gda.pl

$e = u + \frac{\mathbf{v}^2}{2}$	–	specific density energy
$\mathbf{e}_i$	–	unit vector (versor)
$i = x, y, z$	–	the Cartesian coordinates
$\mathbf{I}$	–	unit tensor
I	–	volumetric rate of nucleation
$\mathbf{J}_k$	–	diffusive flux of k,
$\mathbf{J}_\varepsilon$	–	diffusive flux of ε
$\mathbf{J}_a$	–	diffusive flux of a
$\mathbf{J}_x$	–	diffusive flux of x
k	–	turbulent kinetic energy
Ma	–	Mach number
$\mathbf{v} = v_i \mathbf{e}_i$	–	velocity
p	–	pressure
$\bar{r}$	–	is an average radius of droplet
$\mathbf{r}*$	–	Kelvin-Helmholtz critical droplet radius
$\mathbf{q}^c$	–	total heat flux
$S_k, S_\varepsilon, S_x, S_a$	–	source of k, source of ε, source of x and source of a, respectively
T	–	temperature
t	–	time
x	–	dryness fraction

Greek symbols

α	–	volume fraction of condensate
ε	–	turbulent dissipation energy
ρ	–	continuum density
ρ_l	–	density of condensed phase
$\boldsymbol{\tau}^C$	–	total viscous stress

Subscripts

$inlet$	–	inlet condition
$outlet$	–	outlet condition

1 Introduction

Phase transformations, taking place in the water, are a subject of our everyday experience. They happen spontaneously or are initiated by a man in a various kinds of machines and devices. The most interesting phenomenon, occurring in this fluid, is condensation. This phenomenon can be initiated through a rapid pressure change, therefore this is a stress induced phase transitions brought about the mechanism of local tension of the fluid.

In the low-pressure part of steam turbine, the steam state path usually crosses the saturation line in penultimate stages [4, 5] and steam condensates creating tiny droplets. The formation and evolution of these droplets has lower the performance of the wet turbines stages and their effects on

the efficiency are collectively known as wetness losses [4]. Nowadays, due to work of steam turbines at a partial load, process of homogeneous and heterogeneous condensation still is observed. Nevertheless, thermomechanical aspects of the nucleation, growth and interaction of water droplets in the steam turbine of large output are still poorly understood [1,2]. It is because, that the flow in the low-pressure part of steam turbine is complicated and still requires thorough experimental and numerical analysis.

One of the most unwanted effect of turbine operation in low pressure conditions, is related to nonequilibrium condensation [1,5]. Steam enters the low-pressure (LP) turbine as superheated vapor and leaves saturated, with wetness forming as a result of several phase transition processes. The wetness mainly consists of large number of minute droplets which are initially nucleated within and generally carried by the flow [7–9]. As far as phase transitions are induced by the pressure drop, these do not always occur in the vicinity of the saturation line. According to the rate of pressure drop and the steam quality, these phase transitions can occur far from equilibrium conditions. In such situation the basic questions are focused on inception and growth of water droplets due to homogenous and heterogeneous condensation [1,5]. Several observations confirm however, that condensation often occurs earlier than it is predicted by theory, i.e., before the Wilson line. It is because the nucleation can start at some soluble and insoluble impurities, particle of dust, chemical compounds or corrosion products [5,6].

Liquid phase in the flowing vapor through stages of the steam turbine is the cause of a lot of failures [6]. The formation and evolution of these droplets lower the performance of the wet stages of the turbines, and their effects on the efficiency are collectively known as wetness losses [7–9]. Droplets of condensed phase can move with velocity different than gas phase velocity and can seriously damage blades. Erosion of rotor blade leading edge is mainly due to droplets that form behind the trailing edge of guide vanes [5,6]. Nowadays, due to work of steam turbines at partial load, process of homogeneous and heterogeneous condensation still is observed [6]. The formation of drops of condensate under conditions other than nominal operation of turbine is a process still unknown. Engineers and designers involved in the development of power station machines using condensable working fluids, have a need to better understand the impact of moisture formation on a machine performance and its lifetime. In meeting this interest the large-scale experiments and measurements are generally most signifi-

cant and required if the technical process is to be considered [6].

The first time the de Laval nozzle has been used in steam turbines in 1888. Nowadays nozzles are commonly used to acceleration different fluids in various technical devices. In the space between the turbine blades, which resembles the shape of the de Laval nozzle, the shock wave can appear, which has a negative impact on the flow of water vapour. Shock wave is the result of interaction between a normal shock wave and the boundary layer, which produces a λ-foot structure. It is well-known and experimentally confirmed that for low Mach numbers the λ-feet are of the same size at both nozzle walls. However, at higher velocities (Mach number, Ma > 1.4) the λ-feet generated on the upper and lower walls of a symmetric nozzle become different in size. Flow separation inside propulsive nozzles generates unsteady and asymmetrical shock structures and induce fluctuating side loads which potentially can damage the structure. It has also been observed that the tendency towards asymmetry depends on the nozzle divergence angle [10–13]. The most of the experimental data used for validation of the numerical models are relatively old, and do not include a precise investigation of the shock wave behaviour in the wet steam regime.

In the present paper we have focused on the precise prediction of the spontaneous condensation phenomena in wet steam flow. Novelty of our approach lies on modelling both the moment of initiation of a phase transition, as well as the moment of its reverse progress – called here revaporization of the condensate phase. In the paper some original mechanistic model of droplet evaporation is involved, numerically implementated and compared with the experiment carried out by Dykas in 2013 on the half arc nozzels [3]. The model of a single continuum with a special microstructure growing up during phase transitions, proposed by Bilicki and Badur, is taken to be a general no equilibrium framework for description of condensation as well as vaporization. Evaporization, in our model is governed not only by mass transport but also by internal structure energy that is based on balance of heat energy transported into a droplet.

2   Conditions of experiment

The Silesian experiment was carried out on two half arc de Laval nozzles of 'rectangular' cross-section. The D1 half nozzle is an arc nozzle with wall curvature radius of 700 mm and critical throat height of 55.5 mm. The D2 nozzle, is also an arc nozzle with lower critical throat height of 27.5 mm.

Wall curvature radius of D2 nozzle is about 525 mm. The width of the flow channel is 110 mm [3]. The shape of two half arc de Laval nozzles is shown in Fig. 1. Superheated steam with very stable parameters was supplied from the 1 MW boiler. The parameters ahead of the test section was controlled by means of a control valve and desuperheater, providing the steam with parameters corresponding to the conditions prevailing in low-pressure turbine stages. The static pressure measurement in the nozzles was carried out at a distance of 200 mm downstream from the critical throat, along the center line of the nozzle width. The distance between pressure taps was 10 mm [3].
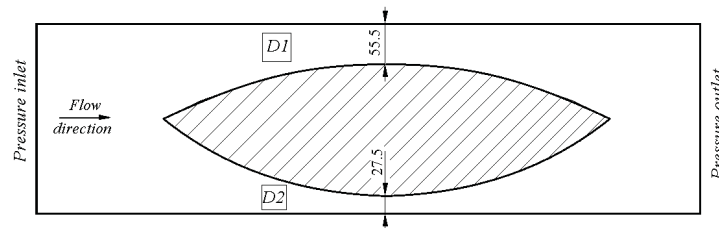
Figure 1: The geometries of two half arc de Laval nozzles [3].

3   Conditions of numerical analysis

Modeling conditions have been taken from description of experiment [3] that was conducted at the Institute of Power Engineering and Turbomachinery of the Silesian University of Technology site. Inlet total pressure was $p_{inlet} = 0.96 \times 105$ Pa, inlet temperature $T_{inlet} = 381$ K. Back pressure at the nozzle outlet was about $p_{outlet} = 0.4 \times 10^5$ Pa. These boundary conditions correspond to experimental conditions for case of D1 nozzle [3]. For the purposes of the problems considered in this paper it has been assumed that the steam is perfectly pure. Mesh for full geometry of the nozzle (Fig. 2) has consisted of 390 000 hexahedral finite volumes.

4   Governing equations of employed CFD model

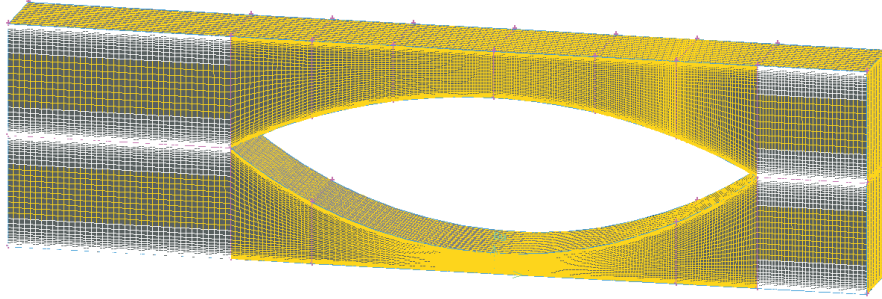For our model governing equations are based on the following balance of liquid-vapour mixture:

Figure 2: FVM discretization of two half arc de Laval nozzles.

- balance of mass – ρ:

$$\partial_t(\rho) + \operatorname{div}(\rho\mathbf{v}) = 0 \,, \tag{1}$$

- balance of momentum – $\rho\mathbf{v}$:

$$\partial_t(\rho\mathbf{v}) + \operatorname{div}(\rho\mathbf{v} \otimes \mathbf{v} + p\mathbf{I}) = \operatorname{div}(\boldsymbol{\tau}^C) + \rho\mathbf{b} \,, \tag{2}$$

- balance of energy – e:

$$\partial_t(\rho e) + \operatorname{div}(\rho e\mathbf{v} + \rho\mathbf{v}) = \operatorname{div}(\boldsymbol{\tau}^C\mathbf{v} + \mathbf{q}^C) + \rho\mathbf{b}\mathbf{v} \,, \tag{3}$$

- turbulence energy evolution – k:

$$\partial_t(\rho k) + \operatorname{div}(\rho k\mathbf{v}) = \operatorname{div}(\mathbf{J}_k) + \rho S_k \,, \tag{4}$$

- turbulence dissipation evolution – ε:

$$\partial_t(\rho\varepsilon) + \operatorname{div}(\rho\varepsilon\mathbf{v}) = \operatorname{div}(\mathbf{J}_\varepsilon) + \rho S_\varepsilon \,, \tag{5}$$

- evolution of wetness fraction – x:

$$\partial_t(\rho x) + \operatorname{div}(\rho x\mathbf{v}) = \operatorname{div}(\mathbf{J}_x) + \rho S_x \,, \tag{6}$$

- evolution of number of droplets – a:

$$\partial_t(\rho a) + \operatorname{div}(\rho a\mathbf{v}) = \operatorname{div}(\mathbf{J}_a) + \rho S_a \,. \tag{7}$$

An additional balance equations for k, ε and x are related to the evolution of turbulence in the condensing flow, or the condensation evolution under turbulent flow condition. Both are fully nonequilibrium phenomena, that should be combined by the sources S, and thermodynamical forces which constitute the fluxes $\mathbf{J}$. The above set of nine equations is to be integrated within every finite volume [5, 10, 11].

Process of growth of individual droplet is governed by mass, momentum and energy transport mechanism between gas and liquid phases. Droplet growth can be described by an evolution of radius of droplet that moves in the wet steam field. Models are needed when nucleation start at some particles, dust, chemical compounds or corrosion products, that often happens before a Wilson line. Other sources of droplets are related to the mechanical action of steam flow and water film at surface of blades [1, 5]. The dryness fraction sources S_x (in Eq. 6) can be divided into homo- and heterogeneous sources of the mass generation rate due to condensation and evaporation. Homogenous source includes part responsible for inception of droplets and part responsible for growth and evaporation of droplets:

$$S_x = \frac{4}{3}\pi \rho_1 \, \mathrm{I} \mathrm{r}_*^3 + 4\pi \rho_1 \alpha \, \bar{\mathrm{r}}^2 \frac{\partial \bar{\mathrm{r}}}{\partial t} \,, \tag{8}$$

where: $\bar{\mathrm{r}}$ – is an avarage radius of droplet, ρ_1 – density of condensed phase, r_* – the critical Kelvin – Helmholtz radius of droplet, I – is a volumetric rate of nucleation, α – volume fraction of condensate [1, 2, 7, 8]. Other details of our model have been presented in the articles [1,5,7,8].

5   Results and discussion

Figure 3 shows a comparison of the static pressure distribution obtained from numerical simulation with experimental data (case of D1 nozzle). This model of condensation provides a good agreement with experiment. Schlieren pictures were carried out during the experimental campaign to improve the possibility of identifying shock wave. In the Fig. 4 we can see photo of shock wave taken during experiment and the same shape and localization of shock for computational fluid dynamics (CFD) simulation for the same flow conditions. The calculated distribution of the wetness fraction (Fig. 5) shows partial evaporation of the liquid phase on the shock wave.

In considered case a velocity of steam is very high (Ma > 1.4), therefore size of λ-feet generated on the upper and lower walls is different. Additional
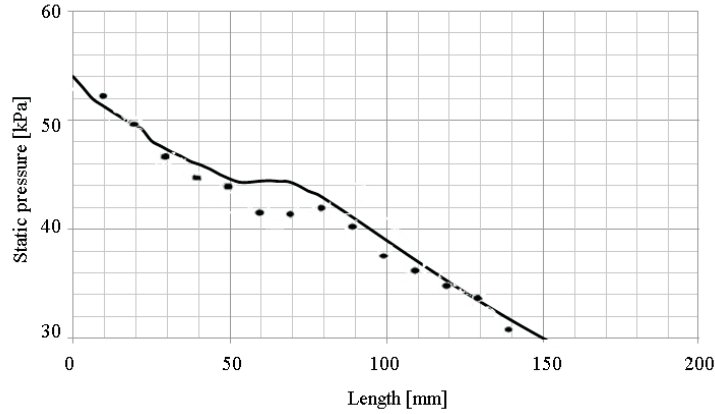
Figure 3: The static pressure distribution along straight wall of the D1 nozzle, comparison of the numerical results (solid line) with experiment data (dots).
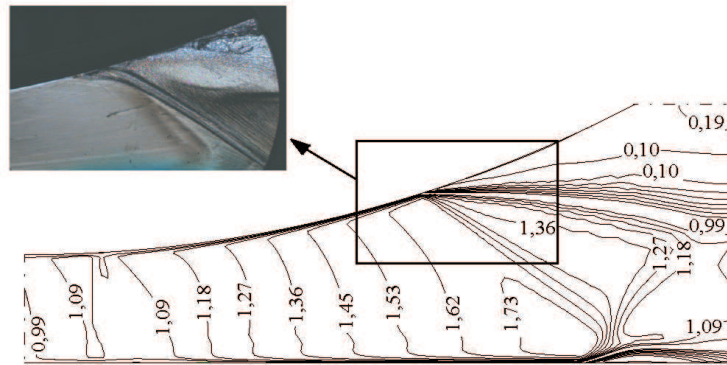

Figure 4: Calculated Mach number distribution and Schlieren pictures from experiment for D1 nozzle [3].

asymmetry is enhanced by different shape of walls. The λ-feet is a result of interaction between a normal shock wave and the boundary layer. The shock/boundary layer interaction produces two separated flows: 1 – without reattachment downstream for upper wall (separation this is a free shock separation) and 2 – with reattachment downstream for lower straight wall (this is a restricted shock). The interaction between the two oblique shocks (C1 and C3 in Fig. 6) forms a Mach disc (MD). The λ-shock structures C1 – C2 and C3 – C4 are jointed to Mach disc by two triple points T1 and T2.
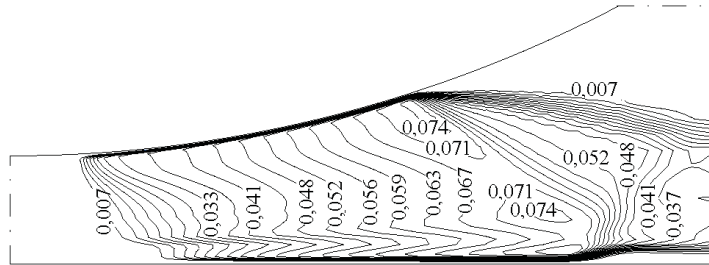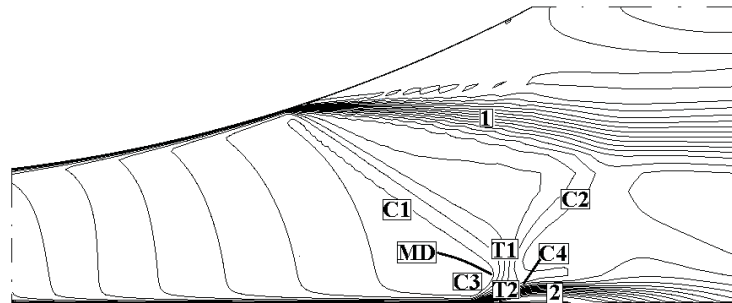
Figure 5: Calculated wetness fraction for D1 nozzle.

Figure 6: Distribution of Mach number – asymmetrical shock pattern for Ma > 1.4.

For a given de Laval nozzle geometry authors have conducted calculations for wet steam model. It was decided to increase the pressure on both the inlet and outlet by the value of 10^5 Pa. Our numerical investigation have shown that for new boundary conditions the shock wave oscillates with frequency 72.3 Hz. Location of the shock wave at various time points for new boundary conditions is shown in Fig. 7.

Two cases are considered for the same parameters of the inlet: $p_{inlet} = 1.8 \times 10^5$ Pa, $T_{inlet} = 415$ K. For case A back pressure at the nozzle outlet was about $p_{outlet} = 0.7 \times 10^5$ Pa, for case B, it was decided to increase the outlet pressure to $p_{outlet} = 1.3 \times 10^5$ Pa. Figure 8a shows the calculated distribution of the wetness fraction for case A. For this case evaporation of condensate on the shock wave is slight. Increasing the back pressure causes enhancement the evaporation of the condensate droplets in the shock wave zone, what we can see in the Fig. 8b.
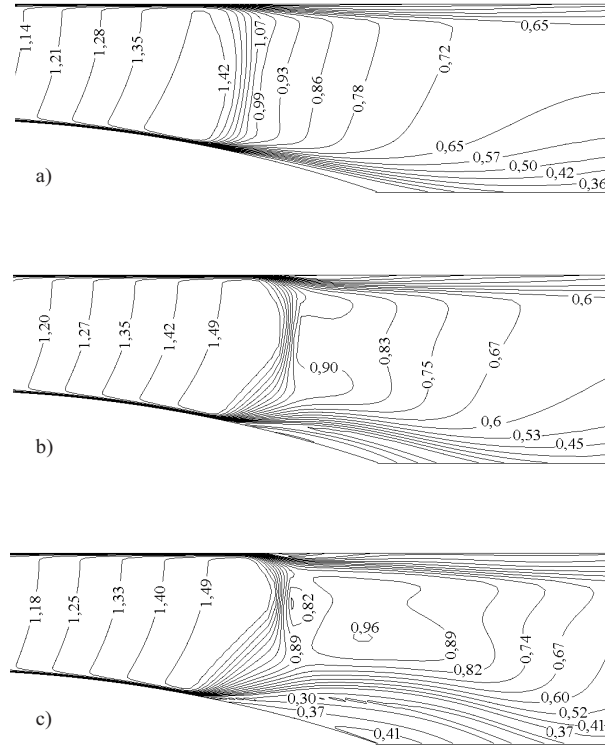
Figure 7: Distribution of Mach number for different moments of time: a) in time t, b) in time $t + 0.004$ s, c) in time $t + 0.008$ s.

6   Conclusions

The proposed model of nineequation non-equilibrium have been tested and compared with the experimental data. This wet-steam model, describing both condensation and revaporization, applied to de Laval nozzle gives satisfactory results that agree well with experimental data. Presented data indicates correctness and utilization of employed model for condensing flows in more complex geometries. In considered case (boundary conditions for D1 nozzle) a velocity of steam is very high (Ma > 1.4), therefore size of λ-feet generated on the upper and lower walls is different. This phenomena is depending on interaction between a normal shock wave and the boundary layer. Additional asymmetry is enhanced by different shape of walls. Our numerical investigation have shown that for new boundary conditions (in-
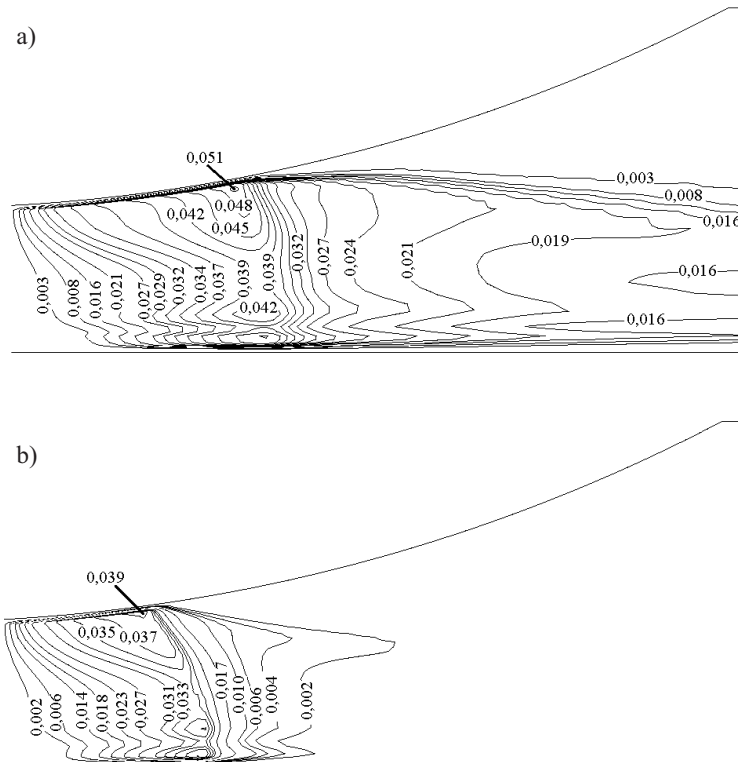
Figure 8: Calculated wetness fraction: a) slight evaporation for case A, b) enhancement evaporation for case B.

crease the pressure on both the inlet and outlet by the value of 10^5 Pa) the shock wave oscillates. Increase pressure at the outlet side causes enhancement evaporation of condensate in the shock wave zone.

References

[1] Biliński Z., Badur J.: *A thermodynamically consistent relaxation model for a turbulent, binary mixture undergoing phase transition.* J. Non–Equilibrium Thermodyn. **28**(2003), 145–172.

[2] Kornet S., Badur J.: *An asymmetrical λ-foot of condensing steam flow in the IFFM PAS nozzle.* J. Phys.: Conf. Ser. **530**(2014), 012018, 1–8.

[3] Dykas S., Majkut M., Smołka K., Strozin M.: *Research on steam condensation flow in nozzle with shock wave.* J. Power Technol. **93**(2013), 288–294.

[4] Puzyrewski R.: *Theoretical and experimental studies on formation and growth of water drops in LP steam turbines.* Transactions IFFM **42–44**(1969), 289–303.

[5] Karcz M., Zakrzewski W., Lemański M., Badur J.: *Issues of 3D modeling the spontaneous condensation part of the low pressure steam turbine of 200 MW.* In: Proc. 10th Conf. of Science and Technology 'Thermal Power Upgrades-Operation-Maintenance' , Słok, near Bełchatów 2001, 253–262 (in Polish).

[6] Kornet S., Badur J.: *'Eulerian – Eulerian' versus 'Eulerian – Lagrangean' models of condensation.* Logistyka **4**(2014), 4463–4473.

[7] Zakrzewski W., Karcz M., Kornet S.: *Estimatiom of the steam condensation flow via CFD methods.* Transactions IFFM **112**(2012), 1–12.

[8] Zakrzewski W., Nastałek L., Badur J., Jesionek K., Straś K., Masłyk M.: *Modeling of the Baumann turbine stage operations, Part I. Flow.* Arch. Energ. **32**(2012), 2, 24–23.

[9] Banaszkiewicz M., Badur J. : *Gradient theory for the description of interfacial phenomena.* TASK Quart. **4**(2000), 213–290.

[10] Namieśnik K., Doerffer P.: *Numerical simulation of shock wave patterns in supersonic divergent symmetric nozzles.* TASK Quart. **9**(2004), 53–63.

[11] Bourgoing A., Reijasse Ph.: *Experimental analysis of unsteady separated flows in a supersonic planar nozzle flow.* Shock Waves **24**(2006), 251–258.

[12] Sellam M., Fournier G., Chpoun A., Reijasse Ph.: *Numerical investigation of overexpanded nozzle flow.* Shock Wave **24**(2014), 33–39.

[13] Verma S. B., Manisanka C.: *Origin of flow asymmetry in planar nozzle with separation.* Shock Wave **24**(2014), 191–209.